Construction and Building Materials 211 (2019) 271–283

Contents lists available at ScienceDirect

Construction and Building Materials

journal homepage: www.elsevier.com/locate/conbuildmat

Development of fly ash/slag based self-compacting geopolymer concrete using nano-silica and steel fiber

Mehmet Eren Gülşan [a,*], Radhwan Alzeebaree [b,c], Ayad Ali Rasheed [a], Anıl Niş [d], Ahmet Emin Kurtoğlu [d]

[a] Department of Civil Engineering, Gaziantep University, Gaziantep, Turkey
[b] Akre Technical Institute, Duhok Polytechnic University, Duhok, Iraq
[c] Department of Architecture, Nawroz University, Duhok, Iraq
[d] Department of Civil Engineering, İstanbul Gelisim University, Istanbul, Turkey

HIGHLIGHTS

- Simultaneous use of nanosilica(NS) and steel fiber(SF) improves flexural properties.
- All self compacting geopolymer concrete mixes (SCGC) were in VS2/VF2 viscosity class.
- Mixes including NS were observed to be more cohesive than mixes without NS.
- Simultaneous use of NS and SF did not reduce compressive strength of SCGC specimens.
- Statistical analysis showed amount of influence of SF and NS on properties of SCGC.

ARTICLE INFO

Article history:
Received 29 June 2018
Received in revised form 15 March 2019
Accepted 18 March 2019
Available online 25 March 2019

Keywords:
Self-compacting geopolymer concrete (SCGC)
Fresh state properties
Nano silica
Steel fiber
Bonding strength
Flexural toughness

ABSTRACT

This study investigates the simultaneous effect of nano-silica and steel fiber on the fresh and hardened state performance of self-compacting geopolymer concretes (SCGC). For this purpose, self-compacting geopolymer concretes without and with nano-silica (0, 1% and 2%), and without and with steel fiber (0, 0.5% and 1%) were produced. Hooked-end steel fibers were used with a length of 30 mm and an aspect ratio of 40. Self-compacting geopolymer mixes were produced using 50% fly ash (FA) and 50% ground granulated blast furnace slag (GGBFS) with a constant alkaline activator to binder ratio of 0.5. For the alkaline activator, sodium silicate solution (Na_2SiO_3) and sodium hydroxide solution (NaOH) were utilized with a ratio (Na_2SiO_3/NaOH) of 2.5. Fresh state experiments were carried out via slump flow, L-Box, and V-funnel tests, while hardened state experiments were conducted using compressive strength, flexural strength, and bonding strength tests to estimate the effects of nano-silica and steel fiber together on the resulting performances of SCGC specimens. Test results were also evaluated statistically in order to clarify the contributions of the important parameters on the resulting performance. Moreover, correlations between the experimental data were studied to investigate the relationships between the fresh and hardened state performances. The results demonstrated that incorporation of nano-silica and steel fiber affected the fresh state properties adversely; however, a combined utilization of them improved bond strength and flexural performance of the SCGC specimens significantly. In addition, the effect of nano-silica was found to be dominant on fresh state properties and compressive strength, while the effect of steel fiber was found to be superior on flexural performance and bonding strength.

1. Introduction

Concrete is the most commonly used structural material due to the availability of raw materials and ease of shaping. However, significant amount of greenhouse gases (CO_2, etc.) are released to the environment due to the combustion of fossil fuels and the decarbonization of limestone during the cement production process. In addition, after aluminum and steel material, ordinary Portland cement (OPC) can be considered as the most energy requiring material [1,2]. Therefore, the negative impacts of CO_2 on the environment and the high amount of required energy are significant issues for both cement industry and future of mankind. New enviroment-friendly structural materials should be utilized instead of ordinary concrete to cope with environmental problems [3,4]. Recently, the geopolymer concrete has started to emerge as an

* Corresponding author.
E-mail address: gulsan@gantep.edu.tr (M.E. Gülşan).

https://doi.org/10.1016/j.conbuildmat.2019.03.228
0950-0618/

environment-friendly concrete as an alternative to ordinary (OPC) concrete [5–7]. Geopolymer concretes have received vast amount of attention due to the significant reduction in both the amount of CO_2 release and necessity of natural resources. Unlike to OPC, the manufacture of the raw materials does not require a calcining process leading to reduction in the energy consumption. It is pointed out in literature that amount of CO_2 release of the geopolymer concrete is 5–6 times lower as compared to the OPC concrete [8,9]. Furthermore, the usage of geopolymer concrete not only decreases the CO_2 emissions considerably, but also uses the by-product wastes of the alumino-silicate composition to fabricate innovative construction materials [10,11].

Self-compacting concrete (SCC) is commonly utilized for the construction of civil engineering structures, especially in pre-cast industries, high rise buildings and structures that need congested reinforcement. The fundamental features of SCC are flowability, filling and passing ability without segregation and/or bleeding. Self-compacting geopolymer concrete is a novel idea in the concrete sector. It is an advanced concrete type that includes the properties of both geopolymer concrete and SCC [12–14]. Very few or limited studies have been conducted on self-compacting geopolymer concrete (SCGC). For the potential use, as in the case of ordinary SCC, further investigation is required to evaluate both fresh and hardened state performance of SCGC.

Mineral fillers and supplementary cementitious materials (SCM) are used to decrease the cost, enhance the workability and the hardened state properties of concretes [7,15,16]. Fly ash and GGBFS are used in the literature broadly as an SCM due to the positive contributions of them to mechanical performance of the concrete, environment and economy [11,17].

SCC has poor tensile strength and ductility and steel fibers are generally used to eliminate this drawback [18]. Steel fibers improve the post-cracking, toughness, and ductility of the concrete [19,20]. Furthermore, steel fiber reinforced SCC provides more reasonable costs/benefits ratio as compared to ordinary SCC [21]. The optimization technique and design procedure to achieve the SCC requirements depend on the fiber characteristics as well as the fiber content [12,14,22]. Due to economic considerations, optimum amount of steel fibers is considered as 1% of concrete volume for the majority of structures [23].

Alkali-activated or geopolymer concrete is a green material and also has acceptable hardened state performance. In addition, it requires a lower amount of energy in the production state and releases a lower amount of carbon dioxide as compared to ordinary concrete [24]. Geopolymer is an inorganic binding material and it has become as an alternative material to the OPC [25]. Especially, fly ash based geopolymer concrete can be utilized instead of ordinary cement and it can also adsorb and immobilize toxic and radioactive materials. The mechanical and durability performance of the fly ash based geopolymer concrete are a major concerns in the concrete industry [26]. In addition to fly ash, phosphate sludge [27], waste glass powder [25], red mud [28] were also tried as a raw material for geopolymer production. In literature, it is proposed that waste materials such as, ground granulated furnace slag and silica fume can be utilized to replace fly ash in GPC [25]. As can be seen from the studies, the fly ash based geopolymer concrete is commonly used type of geopolymer concrete, while fly ash can be replaced by slag for production of GPC. Therefore, it can be concluded that investigations regarding geopolymer concrete should be expanded.

The usage of nano silica (NS) in SCC was also studied earlier and started to be used commonly because of the improvements in the performance of SCC. However, studies related with the fresh and mechanical properties of fly ash/GGBFS based SCGC are limited in the literature. Due to the lack of knowledge in the material characterization of geopolymer concretes, geopolymer concretes are not included in the structural design codes and structural applications. Additional study is needed to improve the knowledge regarding the fresh and mechanical properties of the self-compacting geopolymer concrete. Therefore, the aim of this study is to investigate the simultaneous influence of NS and steel fiber on the fresh and mechanical performance of the SCGC specimens.

2. Experimental procedure

2.1. Materials

Nine types of self-compacting geopolymer mixture (SCGC), without and with NS (0, 1 and 2%), and without and with SF (0, 0.5 and 1%) were produced to analyze the simultaneous effect of NS and SF on the fresh and mechanical performances of SCGC. F-type fly ash (FA) according to ASTM C 618 and GGBFS were used as binder materials in current research. The crushed limestone with maximum particle sizes of 11 mm and 4 mm were utilized as coarse and fine aggregates, respectively. Alkali activator was a mix of sodium silicate (Na_2SiO_3) and sodium hydroxide solutions (NaOH). The sodium silicate was obtained from the regional source (Na_2O:13.7%, SiO_2: 29.4, water: 55.9% by mass). The sodium hydroxide had 97–98% purity and its molarity was selected as 12 M which had been proposed to obtain reasonable mechanical performance for SCGC in another research. [29]. Table 1 shows the properties of fly ash, GGBFS, and nano-silica used in the study.

The hooked-end steel fibers with two steel fiber ratios (0.5% and 1%) were used in the study and steel fibers have a length of 30 mm and an aspect ratio of 40 [19,30]. A polycarboxylates ether based superplasticizer with a density of 1.095 g/cm^3 was used to obtain high flowability without segregation and/or bleeding [31,32]. In addition, ribbed steel reinforcements with a diameter of 16 mm and a minimum yield strength of 420 MPa were used to investigate the combined influence of SF and NS on the bonding strength of the specimens.

2.2. Mix design

Different series of SCGC mixtures were produced with a constant total binder amount of 450 kg/m^3. The mixtures contain 50% fly ash and 50% slag by weight. The nano-silica was incorporated with ratios of 1% and 2% by weight of the binder. Steel fibers were utilized with amounts of 0.5% and 1% by volume of the concrete similar to the previous study [33]. Table 2 illustrates the amount of each component as weight for 1 m^3 concrete. For mixture designations, SF indicates the steel fiber, the number next to SF (0-0.5-1) indicates steel fiber ratios, NS indicates the nano-silica, and the number next to NS (0-1-2) indicates ratio of nano-silica.

Aggregate, binder and alkaline amount, maximum grain size (D_{max}), length, volumetric ratio and aspect ratio of steel fiber affect both fresh and mechanical performance of SCGC specimens. The Na_2SiO_3/NaOH ratio lies in the range of 1.5–2.5 for economic reasons [34] and it was utilized as 2.5 in current research.

For the mixing procedure, coarse and fine aggregates, FA and GGBFS were blended for 2.5 min. The alkali activator, superplasticizer, and extra water were added to the mixture in one minute and mixed during additional 2 min. Thereafter, fresh concrete was further mixed during 3 min to ensure homogeneity and uniformity.

2.3. Fresh state tests

After mixing, fresh state tests were conducted on the SCGC mixes, since these mixes should fulfill the flowability and passing ability requirements without segregation and/or bleeding. The flowability of geopolymer SCC specimens was measured via slump flow and V-funnel tests; passing ability was measured using the L-Box test according to the EFNARC committee [35]. In the slump flow test, flow diameters in x and y directions were measured and t_{500} duration, in which flow diameter reaches to 500 mm diameter, were recorded in the test. In the V-Funnel test, the section was totally filled with concrete, then concrete was let to discharge and discharge time was recorded. The viscosity can be measured indirectly via V-funnel and T_{500} slump flow time tests using the rate of flow. In the L-Box test, the passing ability of the mixes (PL value) between narrow openings of bars (41 ± 1 mm) was evaluated by dividing the concrete height of the horizontal section to the height of vertical section after end of concrete flow. Table 3 illustrates the upper and lower limits for fresh state performance of SCC mixes according to the EFNARC specification [35].

2.4. Curing method of the SCGC

After the production of concretes, specimens were covered by a plastic sheet for 24 h to prevent the evaporation of the alkaline solution. Then specimens were put in an electric oven for 48 h at 70 °C. After the completion of the curing period, samples were demolded and kept in water tank, which was in laboratory environment, until the 28th day after concrete casting. For each experiment, identical three samples were produced and the average of the corresponding experimental result was calculated.

Table 1
Physical and chemical characteristics of FA, GGBFS and NS.

Component	CaO	SiO_2	Al_2O_3	Fe_2O_3	MgO	SO_3	K_2O	Na_2O	LOI	SG	BF (m^2/kg)
FA (%)	1.60	62.33	21.14	7.15	2.40	0.10	3.37	0.38	1.58	2.29	379
GGBFS (%)	34.12	36.40	11.39	1.69	10.30	0.49	3.63	0.35	1.64	2.79418	
NS (%)	–	99.80	–	–	–	–	–	–	<1.00	2.20	–

Table 2
Mixture proportion of self-compacting geopolymer concrete.

Mixture	Binder kg/m^3	Na_2SO_3+NaOH kg/m^3	FA kg/m^3	GGBFS kg/m^3	NS kg/m^3	SF kg/m^3	Fine Agg. kg/m^3	Coarse Agg. kg/m^3	Molarity	SP %	Extra water %
SF0NS0	450	225	225	225	0	0	865.61	742.88	12	5	8
SF0NS1	450	225	225	225	5	0	862.65	740.34	12	5	8
SF0NS2	450	225	225	225	10	0	859.69	737.80	12	5	8
SF0.5NS0	450	225	225	225	0	39.2	865.61	742.88	12	5	8
SF0.5NS1	450	225	225	225	5	39.2	865.61	742.88	12	5	8
SF0.5NS2	450	225	222.8	222.8	10	39.2	865.22	742.54	12	5	8
SF1NS0	450	225	220.5	220.5	0	78.4	864.83	742.21	12	5	8
SF1NS1	450	225	222.8	222.8	5	78.4	865.22	742.54	12	5	8
SF1NS2	450	225	220.5	220.5	10	78.4	864.83	742.21	12	5	8

Table 3
Fresh state test evaluation with respect to EFNARC specification.

Slump flow classes		
Class	Slump flow diameter [mm]	
Slump Flow 1	550–650	
Slump Flow 2	660–750	
Slump Flow 3	760–850	
Viscosity classes		
Class	T_{500} [s]	V-funnel time [s]
VS1/VF1	≤2	≤8
VS2/VF2	>2	9 to 25
Passing ability classes		
PA1	≥0.8 with two rebar	
PA2	≥0.8 with three rebar	

2.5. Hardened state tests

The hardened state tests were carried out to analyze the combined influences of NS and SF on the mechanical performance of the self-compacting geopolymer concretes. Compressive strength tests were conducted on cubic specimens (100 × 100 × 100 mm) using ASTM C39 standard [36]. The bonding strength between SCGC and steel rebar was evaluated according to RILEM RC6 [37]. The top layer of the cubic SCGC samples was capped with gypsum to obtain a smooth surface for uniform load distribution. The pullout specimen details are given in Fig. 1.

The bonding strength of the samples under pullout test, τ, is found using the 1st equation:

$$\tau = \frac{P}{\pi * d * L} \quad (1)$$

where P is the force, d is the diameter (16 mm for the study), L is the embedment length of the steel rebar (150 mm for the study).

Flexural strength tests were conducted on notched 100 × 100 × 500 mm specimens in accordance with RILEM 50-FMC/198 Committee [38] by displacement controlled loading machine. The mid-span deflection of specimens were measured using a linear variable displacement transducer (LVDT). The notches were formed at the bottom middle of the specimens. The width of the notches is of 3 mm and the height of the notches is 40 mm with a notch depth to sample depth ratio of 0.4. The specimens were loaded via displacement control with a rate of 0.02 mm/min. The net flexural strength was evaluated by the 2nd equation [39].

$$f = \frac{3P_{max}L}{2b(d-a)^2} \quad (2)$$

where P_{max} is the maximum force, b is the width of the beam, L is the length of the beam, d is the depth of the beam, and a is the depth of the notch as shown in Fig. 2.

Fracture energy (G_F) represents the energy amount required to create a crack in the matrix and it was calculated by the formula proposed by RILEM [38]:

$$G_f = \frac{(w_o + mg\delta_s)}{A_{lig}} \quad (3)$$

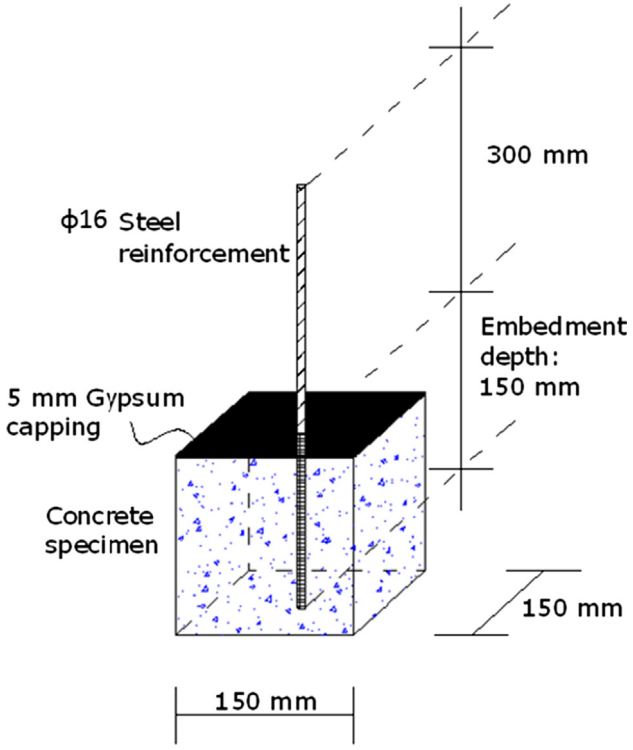

Fig. 1. Test set-up for the bond strength.

where w_o is the area below the force versus displacement behavior, mg is the weight of the specimens, δ_s is the displacement, and A_{lig} is the ligament area.

The critical stress intensity factor (K_{IC}) was determined by the 4th formula [40]:

$$K_{IC} = \frac{3P_{max}l}{2bd^2}\sqrt{a_0}\left(1.93 - 3.07A + 14.53A^2 - 25.11A^3 + 25A^4\right) \quad (4)$$

where P_{max} is the maximum force, l is the clear length of the sample, b is the sample width, d is the sample depth, a_o is the notch depth of the sample, and A is the ratio of notch depth to sample depth.

3. Result and discussions

3.1. Fresh state performance

Flowability and passing ability test outcomes of the SCGC mixes were compatible with the EFNARC specifications [35]. Flow diam-

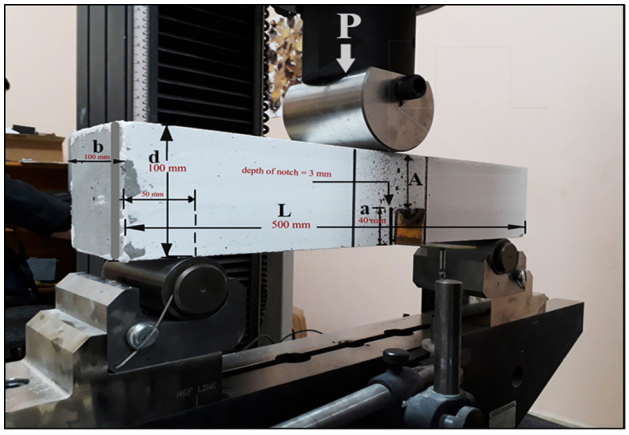

Fig. 2. Test set-up and detail of specimen under three-point bending loading.

eters of SCGC mixes were found to be higher than the minimum flow diameter of 550 mm. No segregation was detected in the SCGC mixes. In addition, resulting slump flow diameters were also compatible with the EN 12350-8 standard [41], which states the minimum slump flow diameter as 600 mm. Effect of NS and SF on fresh state properties of SCGC are analyzed in detail in the following sections by the consideration of each fresh state test separately.

3.1.1. Effect of NS and SF on slump flow diameter

Fig. 3 presents the influence of NS and SF on the slump flow diameter. The highest slump flow diameter (709 mm) was measured for the mix without NS and steel fiber. The incorporation of NS reduced the slump flow diameter of the non-fibrous mixes from 709 mm (without NS) to 695 mm (1% NS) and 680 mm (2% NS). The addition of steel fiber also decreased the slump flow diameter of the mixes without nano-silica from 709 mm (0%SF) to 693 mm (0.5%SF) and 687 mm (1%SF). Decrease in the slump flow diameter due to addition of 2% NS is higher than the decrease due to 1% SF addition.

In addition, the combined effect of NS and SF reduced the slump flow diameter considerably. Therefore, minimum flow diameter of 664 mm was observed for mixes including highest amount of both nano-silica (2%) and steel fiber (1%). Slump flow results indicated that all slump flow amounts were in the range of SF2 class, which are suitable for many structural applications (column, beam or slab) according to the EFNARC specifications [35].

3.1.2. Influence of NS and SF on the slump flow time (T_{500})

Fig. 4 indicates the combined effect of NS and SF on the T_{500} durations, in which elapsed time is recorded until flow diameter of the fresh concrete reaches to 500 mm. For specimens without NS, T_{500} durations of the specimens containing 0%, 0.5% and 1% steel fiber were measured as 2.66 s, 2.72 s, and 2.83 s, respectively. However, for non-fibrous specimens, T_{500} durations of the specimens containing 0%, 1% and 2% nano silica were 2.66 s, 2.98 s, and 3.23 s, respectively. Therefore, it can be concluded that reducing effect of NS on T_{500} duration is higher than the effect of SF. For the specimen containing the highest amount of steel fiber and nano silica (2% NS and 1%SF), T_{500} duration increased to 3.63 s. Similar to slump flow diameter results, higher amounts of T_{500} duration were recorded as a result of simultaneous use of NS and SF. T_{500} duration should be smaller than the value of 6 s according to the EN 12350-8 standard [41]. As a conclusion, T_{500} test results were found to be satisfactory according to both EFNARC specification [35] and EN 12350-8 standard [41].

3.1.3. Influence of NS and SF on V-funnel flow time

The V-funnel flow time is the reflection of the flowability and the viscosity of SCGC. Discharge time from V-funnel sections exhibited similar results with slump flow test results. The discharge times of the specimens without NS were measured as 10.84 s, 12.83 s, and 13.76 s for the 0%, 0.5%, and 1% steel fibrous mixes, respectively. The discharge times for the non-fibrous mixes were 10.84 s (0% NS), 13.24 s (1% NS) and 16.63 s (2% NS). Effect of NS on the discharge time was found to be more than the effect of SF. Similarly, the highest discharge time was observed for the mixes including 2% NS and 1% SF (combined effect) as shown in Fig. 5.a. EFNARC specifications [35] state viscosity classes depending on the V-Funnel and T_{500} slump flow time values, as shown in Fig. 5.b and Table 3.

Based on the test results, all mixes were in the range of VS2/VF2 viscosity class. EFNARC states that VS1/VF1 viscosity class has a good filling ability even for congested reinforcements, but this class is susceptible to bleeding and segregation. VS2/VF2 viscosity class has good bleeding and segregation resistance and low formwork pressure; however, the VS2/VF2 class has an inadequate surface finish properties and it may suffer from the stoppage of flow of SCGC mixes. Results indicated that higher percentage of nano-silica elongated the discharge time, which is beneficial for bleeding and segregation, but it may cause inadequate filling ability. In addition, EN 12350-9 [42] standard states that the discharge time of the V-funnel should be smaller than 15 s to have a good filling ability. The discharge times of the mixes without NS and with 1% NS were below the standard limit value of 15 s, except the mixes including

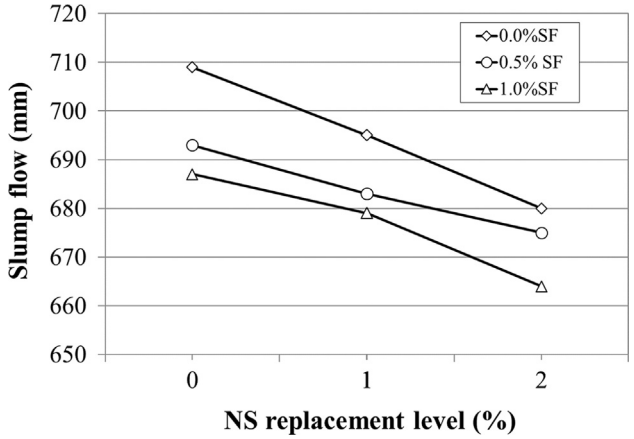

Fig. 3. Influence of NS and SF on the slump flow diameter.

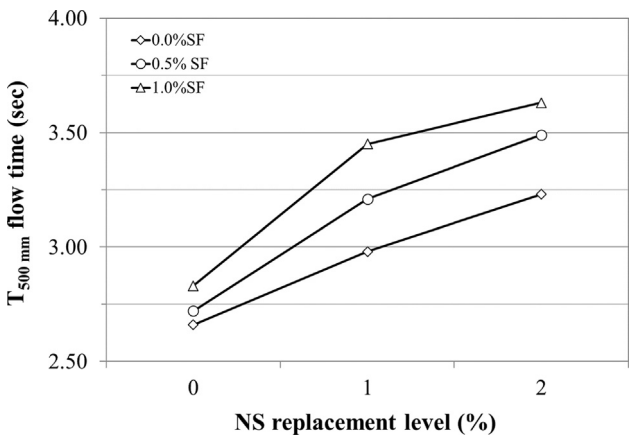

Fig. 4. T_{500} duration versus NS and SF relationship.

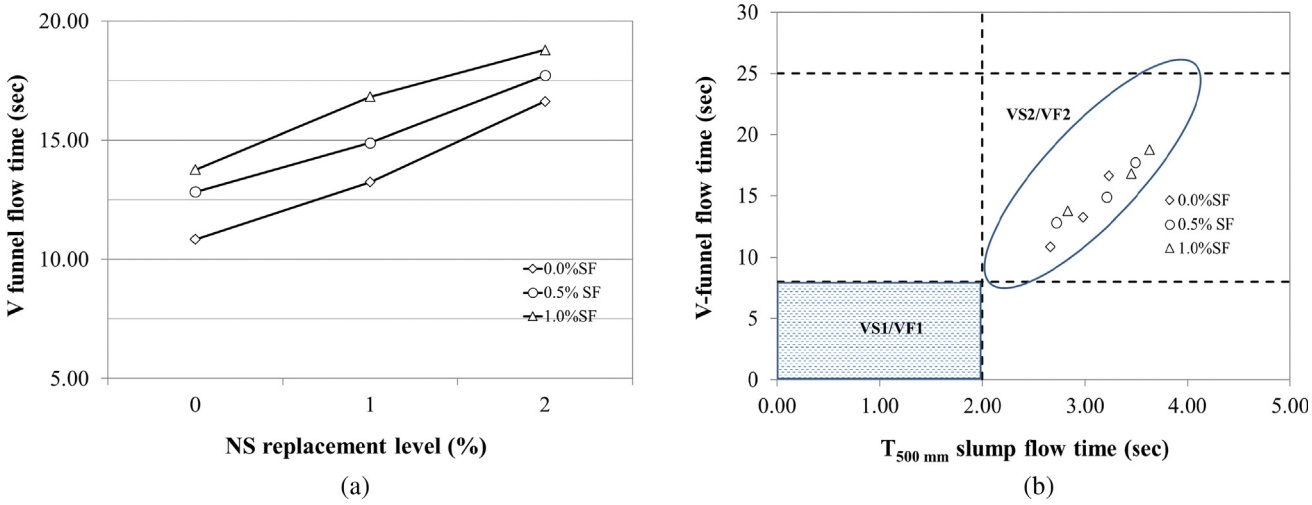

Fig. 5. V-funnel vs the combined effects of NS and SF (a), V-funnel vs T_{500} flow time relationships (b).

1% NS and 1% SF. However, the discharge times of all mixes including 2% NS were higher than the value of 15 s. Therefore, it can be concluded that higher percentages of nano-silica (≥2%) reduce the filling ability of fresh SCGC considerably.

3.1.4. Effect of NS and SF on L-box height

In the L-Box test, passing ability of the mixes (PA or PL value) between narrow openings of three bars (41 ± 1 mm) was evaluated by dividing the concrete heights in horizontal section to the height in vertical section (H2/H1) after end of concrete flow. PL value of SCGC mixes should be equal or higher than 0.8 in order to satisfy adequate passing ability requirements according to both EFNARC specification and EN12350-10 standard [43]. It can be concluded from L-Box test results (Fig. 6) that all mixes have an adequate passing ability (PA ≥ 0.8). The highest passing ability (0.96) was observed for the mixes without NS and SF. PA values of the specimens without NS were 0.96, 0.92, and 0.9 for 0%, 0.5% and 1% steel fibrous mixes, respectively. For the non-fibrous specimens, PA values were calculated as 0.96, 0.91, and 0.88 for the specimens with NS content of 0%, 1%, and 2%, respectively. The incorporation of both NS (2%) and SF (1%) decreased the PA value to 0.82 (lowest PA). It should be noted that further increase in the amounts of NS (>2%) and SF (>1%) may not satisfy the passing ability requirements for the SCGC mixes.

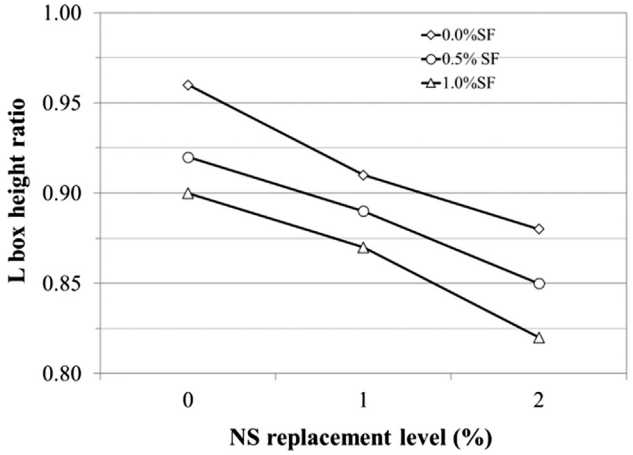

Fig. 6. The L-Box height ratio versus NS replacement level and SF content.

Fresh state results indicated that simultaneous use of NS and SF decreased flowability and passing ability of SCGC mixes. However, even for the highest amounts of NS (2%) and steel fiber (1%) utilized in current study, the self-compacting geopolymer mixes satisfied the required flowability and passing ability criteria as specified by EFNARC specifications and TS EN 12350 standards. Moreover, it was observed that higher amounts of NS improved resistance of SCGC mixes against segregation and bleeding, and the mixes containing NS were observed to be more cohesive than the mixes without NS. The results indicated that fresh state properties of the SCGC mixes decreased as NS and SF contents increased. For the better fresh state performance, the utilization of both NS and SF together should be limited in order to obtain self-compacting geopolymer mixes that have a better flowability and passing ability properties.

3.2. Mechanical properties of SCGC

3.2.1. Compressive strength

Fig. 7 illustrates the effect of NS and SF on the compressive strength of the specimens. Compressive strength of the specimens including NS was lower than the strength of the specimens without NS. This result can be attributed to the unreacted NS which causes an extreme self-dehydration in the mixes leading to formation of cracks and so reduction in compressive strength [44,45]. On the other hand, addition of steel fiber slightly enhanced the compressive strength of the SCGC specimens. The improvement in the compressive strength was found to be more than 5% and 7% for the specimens containing 0.5% and 1% steel fiber, respectively. Similar increases in compressive strength due to the SF inclusions in ordinary concrete were also reported in earlier studies [46–48]. Furthermore, the compressive strength of specimens including NS also improved with the incorporation of SF. Compressive strength values of control specimen (without NS and SF) and the specimen including the highest amounts of NS (2%) and SF (1%) were close to each other. Therefore, it is worth to note that decreasing influence of NS on the compressive strength can be compensated with addition of the steel fiber.

3.2.2. Bond strength

Fig. 8 illustrates the variation in the bond strength of specimens due to the combined effect of NS and SF. It can be said that the bond strength increased significantly with an increase in the SF volume. In addition, NS also improved the bond strength of the

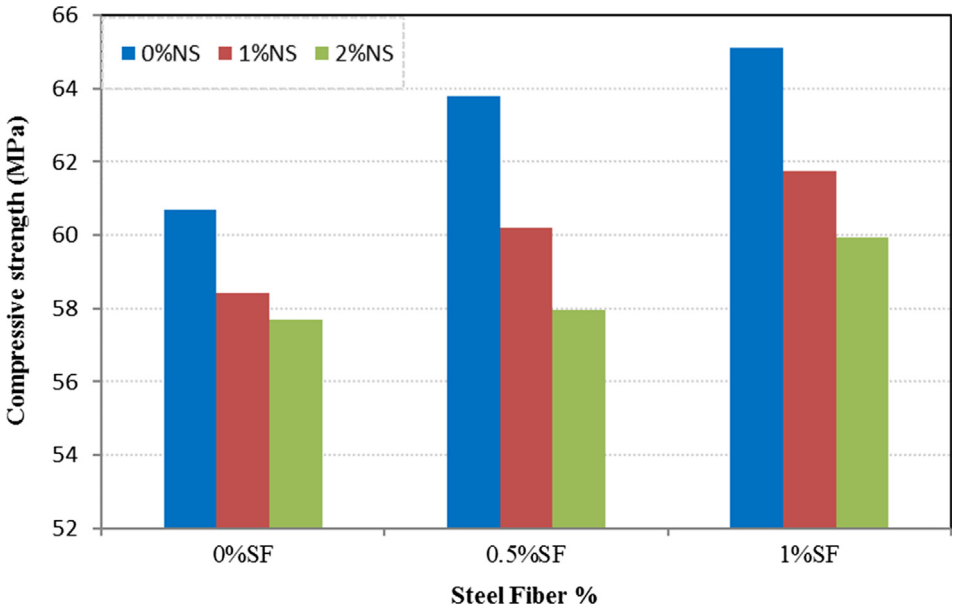

Fig. 7. The influence of NS and SF on compressive strength of the specimens.

SCGC specimens slightly. The highest bond strength enhancement was found to be 25.4% for the specimens including 2%NS and 1% SF as compared to control SCGC specimens. The positive effect of SF on the bonding resistance was more than the effect of NS.

Baran et al. [49] indicated that SF enhanced the pullout strength of strands by controlling the crack development in the concrete samples. They also reported that the confinement level at the strand-concrete interface enhanced with an increase in the SF volume, which improved both friction and the bond strength. They obtained bond strength enhancement as amount of more than 30% due to the steel fiber addition. The researches about the bond strength among steel reinforcement and OPC concrete were conducted; however, there is no or limited study was realized on the bond strength of SCGC specimens including nano-silica. This study may highlight the effectiveness of nano-silica use on the bond strength of the SCGC specimens. In a study [50], researchers stated that the concrete quality is a significant parameter on the bond strength and tensile strain capacity in concrete. Due to the improvement in the quality of the matrix due to the micro-filling effect and pozzolanic activity of NS [20], the NS addition may also enhance the pullout capacity of the reinforced concrete structures.

Fig. 9 illustrates the typical failure patterns of the SCGC specimens after pullout tests. After failure, the rebar was separated from the SCGC specimens without SF; whereas structural rebar remained to survive in the cracked matrix for the steel fibrous specimens. The similar results were also obtained in the earlier study [51] that researchers reported 10–20% improvement in the pullout resistance due to the incorporation of 1% SF by concrete volume. In another research of Harajli and Salloukh [52], the SF reinforced specimens with 2% fiber volume enhanced bond

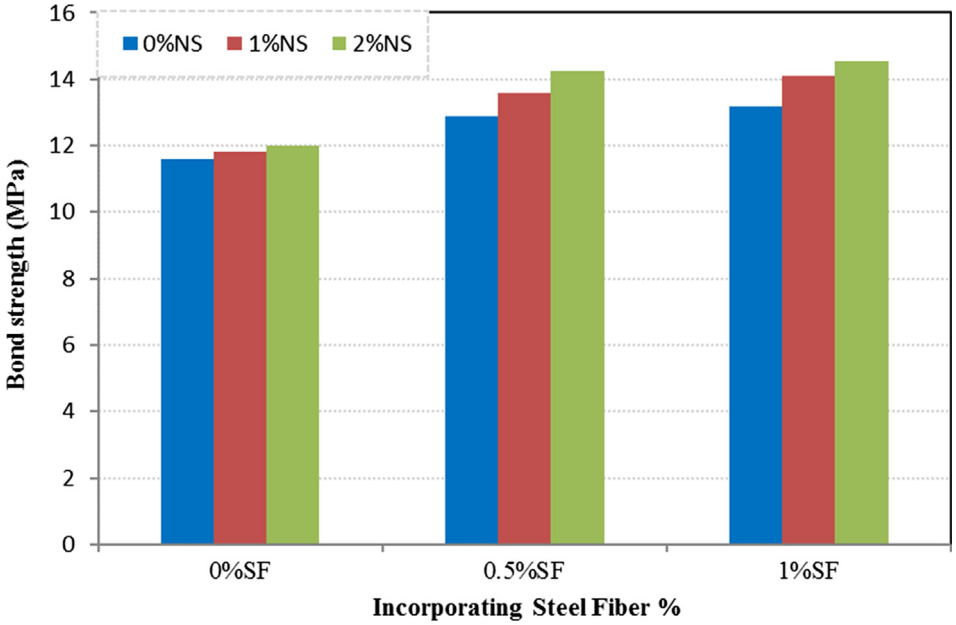

Fig. 8. The combined effect of NS and SF on bond strength.

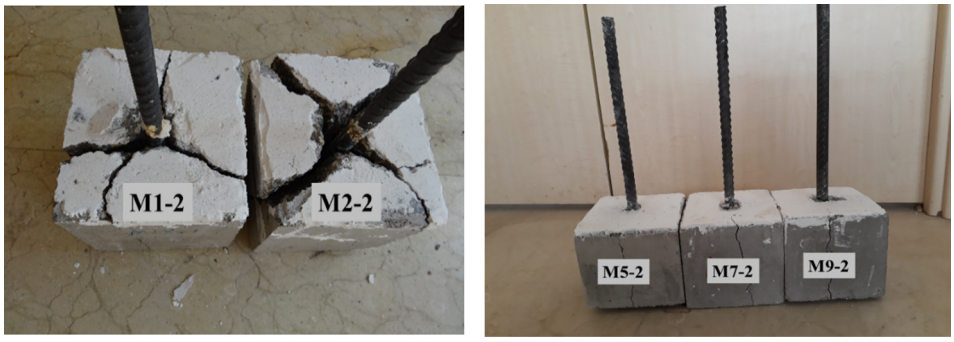

Fig. 9. The fracture patterns of SCGCs: (a) without SF and (b) with SF.

strength up to 55% as compared to non-fibrous specimens. In addition, the bond strength improved more than two or three times when higher steel fiber volume (3–7%) was utilized [52]. Therefore, it can be asserted that the combined utilization of NS and SF enhanced the bond strength of the specimens further due to the crack bridging ability of SF and due to the better adhesion of NS.

3.2.3. Flexural strength

Fig. 10 shows the resulting load-displacement curves of SCGC samples under flexural loading. In the beginning, a linear slope was observed up to the first cracking and after that strain relaxation was observed for all of the GPC samples. The load versus displacement curves of the non-fibrous samples exhibited similar behavior and approximately similar flexural strength values were obtained for these specimens regardless of NS content. When the SF is incorporated and the combined effect of NS and SF was investigated, it was observed that the flexural strength improved with an increase in NS content under the same SF volume concentrations, as shown in Fig. 11. Furthermore, specimens with higher NS and SF contents exhibited lower load relaxations and higher residual flexural strengths as compared to specimens without NS. It may be due to the enhanced bond strength between fiber and matrix due to the NS addition. It can be concluded that simultaneous use of SF and NS achieved the superior bending performance and the maximum flexural strength was obtained for the samples including 2% NS and 1% SF (SF1NS2).

3.2.4. Fracture performance

The area below the load-displacement curve can be estimated by the 3rd equation and the fracture energy results are given in Fig. 12. Similar fracture energy results were obtained for the non-fibrous specimens including different amounts of NS. When the combined effect of NS and SF was investigated, it was resulted that the fracture energy improved with an increase in the amounts of both NS and SF.

The positive effect of SF was due to the crack bridging ability of it, which prevents the opening of cracks and enables further displacement in the SCGC specimens. Meanwhile, NS can improve the bond strength and enhance the adhesion between SF and the matrix. The simultaneous use of both NS and SF exhibited superior fracture performance for SCGC specimens. Another reason for the higher fracture energy results can be attributed to increase in the compressive strength for the specimens including NS and SF as shown in Fig. 7. In a different study, researchers [53] studied the variation of fracture energy in the FA based geopolymer concrete samples and they concluded that fracture energy improved as compressive strength of the samples increased.

The critical stress intensity factor (K_{IC}) of SCGC samples at 28 days was calculated using the 4th equation and the results are given in Fig. 13. The K_{IC} refers to stress intensity required to propagate the crack. Similar critical stress intensity factor results were obtained for the specimens including different NS contents with 0.5% SF. When SF volume increased to 1%, the K_{IC} values increased with an increase in NS volume. More stress was required to open the existing cracks in the specimens when the higher steel fiber volume (1%) and NS volume (2%) were utilized. The increase in the K_{IC} values can be attributed to the higher bond due to the increase in NS content and higher crack arresting capability due to the increase in the SF content.

3.3. Correlation between fresh and hardened performances of SCGC

The correlation of the experimental data is significant for researchers to evaluate the results. Theoretically, the fundamental parameters controlling the fresh state and mechanical performance of concretes are cementitious binder content, w/b, and aggregates. As stated earlier, compressive strength affects most of the mechanical properties of the concrete. In this study, the combined influence of NS and SF on the fresh and mechanical performance of SCGC was investigated. Therefore, the influences of these parameters on the fresh and hardened state performance can be also evaluated via correlating the experimental data each other. It is found that there are close relationships between slump flow and T_{500} time (R^2: 0.8235), L-Box and slump flow (R^2:0.9419), and V-funnel and slump flow (R^2:0.9739), as shown in Fig. 14. The high values of R^2 indicate that slump flow and other fresh state properties are well correlated even in the presence of both NS and SF.

Moreover, there are also noticeably close relationships between slump flow and compressive strength, slump flow and bond strength, and slump flow and fracture toughness, as shown in Fig. 15. The high coefficient of correlation (R^2) values indicate that the mechanical performance of SCGC depends on the slump flow performance of it despite inclusion of NS and SF. Furthermore, acceptable relationships exist between the hardened state properties of the SCGC. The high coefficient of correlation (R^2) values are observed between compressive strength and bond strength, compressive strength and flexural strength, compressive strength and fracture energy, compressive strength and critical stress intensity factor, bond strength and flexural strength, and bond strength and critical stress intensity factor, as indicated in Fig. 16. In general, it can be concluded that there are strong relationships between fresh state and hardened state properties of SCGC specimens despite the inclusion of NS and SF. It can be stated that hardened state properties of the SCGC specimens are highly influenced from the fresh state properties. Therefore, good fresh state performance is inevitable requirement for better mechanical performance for SCGC specimens including both NS and SF.

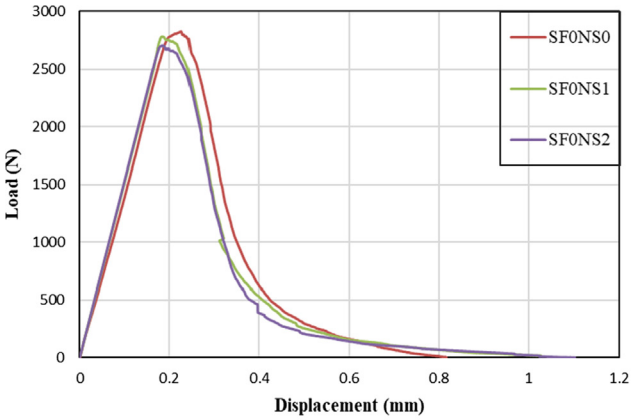

(a) Effect of NS on SCGC mixes without SF

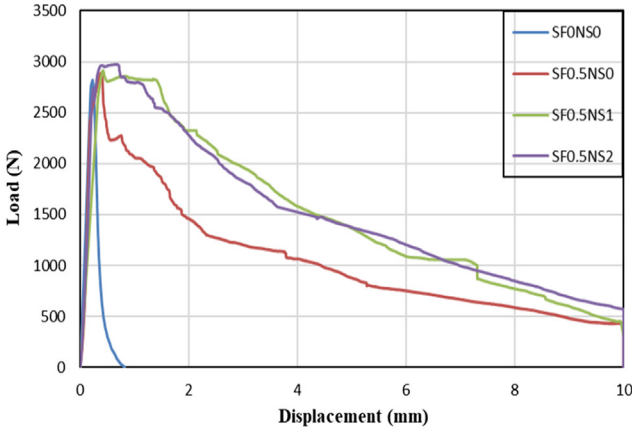

(b) Effect of NS on SCGC mixes with 0.5% SF

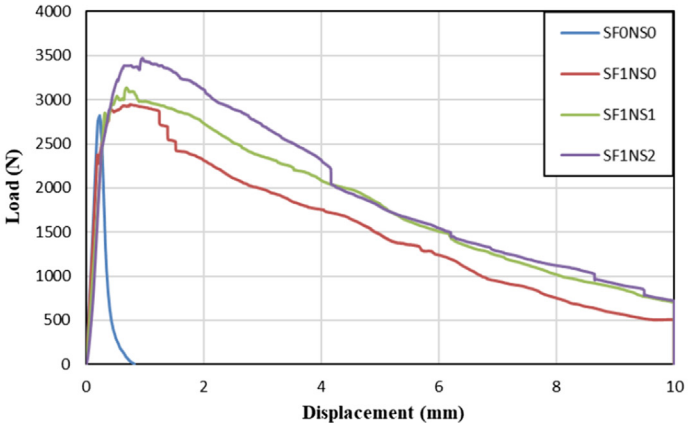

(c) Effect of NS on SCGC mixes with 1% SF

Fig. 10. Effect of GGBFS and SF on load displacement of SCGC.

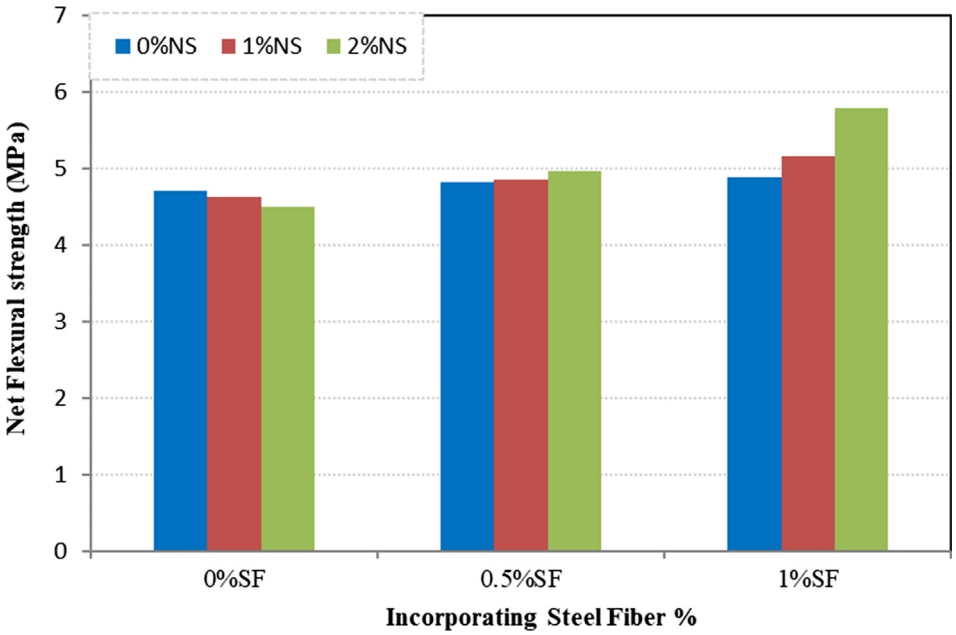

Fig. 11. Effect of NS and SF on the flexural strength.

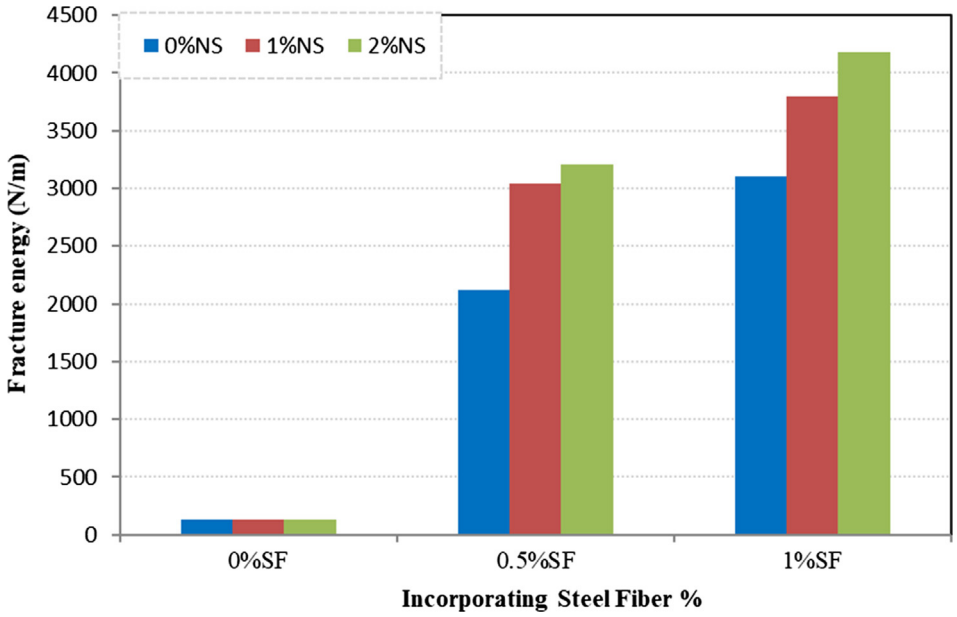

Fig. 12. Effect of combination of SF and NS on Fracture energy of SCGC.

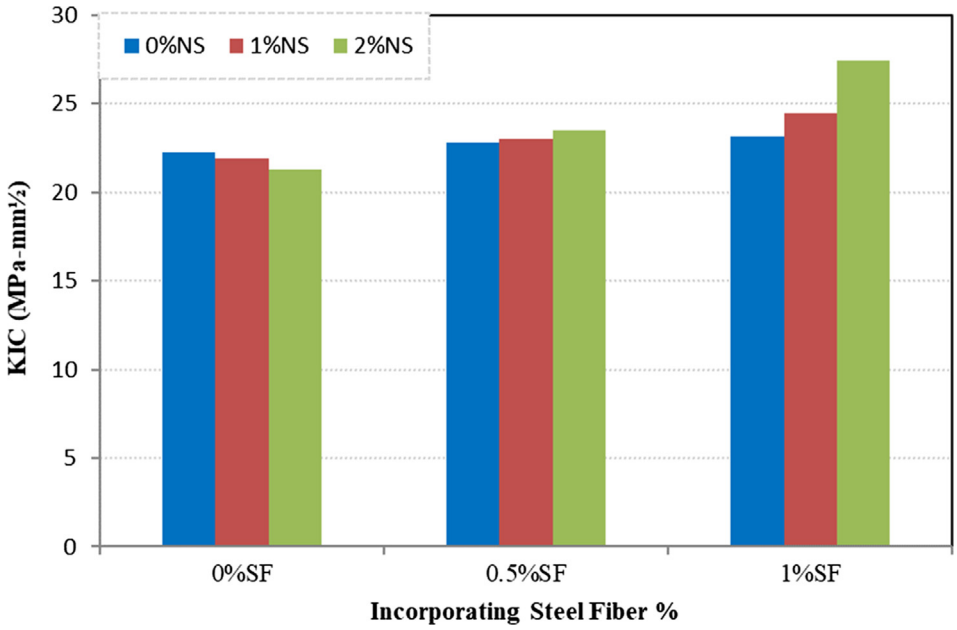

Fig. 13. Effect of NS and SF on the stress intensity factor (K_{IC}).

3.4. Statistical assessment of the self-compacting SCGC specimens

An analysis of variance model with a significant level of 0.05 was carried out to estimate the change in the fresh and hardened properties of SCGC with different levels of NS and/or steel fiber in quantitative form. For this reason, slump flow diameter, slump flow time (T500), V-funnel flow time, L-Box height ratio, compressive strength, bond strength, fracture toughness, flexural strength, and critical stress intensity factor of the concretes were assigned as the dependent variables, while the addition of steel fibers and replacement level of NS were the independent variables. In order to determine significant parameters, a statistical analysis was carried out and p-values were calculated as a result of the analysis. Provided that resulting p-level is smaller than 0.05, this means that the corresponding parameter is a significant parameter for the corresponding property. In addition, percent contribution of each independent parameter was determined to find out the degree of effectiveness of the parameter on the corresponding property. If this value is higher, then it can be concluded that the influence of the parameter on the corresponding property is significant. Table 4 presents the contributions (%) of the parameters to the resulting properties. Statistical analysis results indicate that NS replacement was found to be more effective than the addition of SF regarding fresh state properties (slump flow, V-funnel flow time, T500 flow time and L-Box ratio). Effect of NS on the compressive strength of the specimens is also higher than the effect of SF. However, the addition of SF was found to be more effective as compared to NS replacement regarding bond strength and flexural perfor-

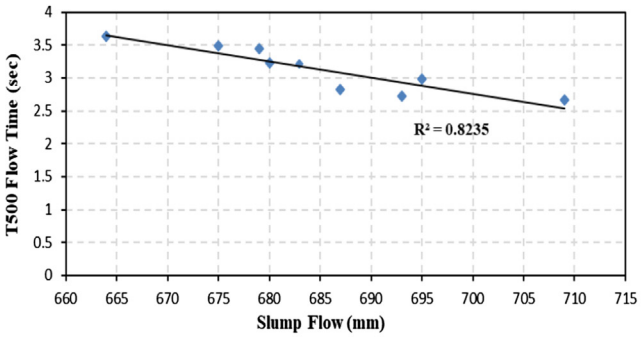

(a) Slump flow versus T_{500}

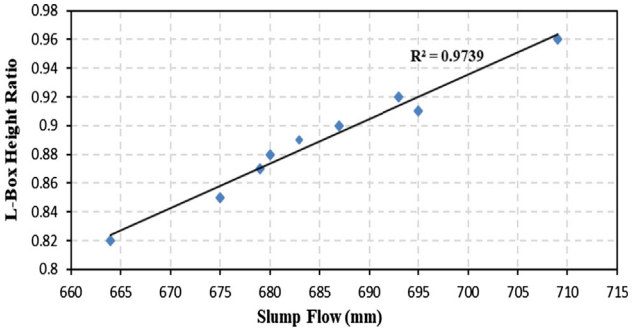

(b) Slump flow versus L-Box

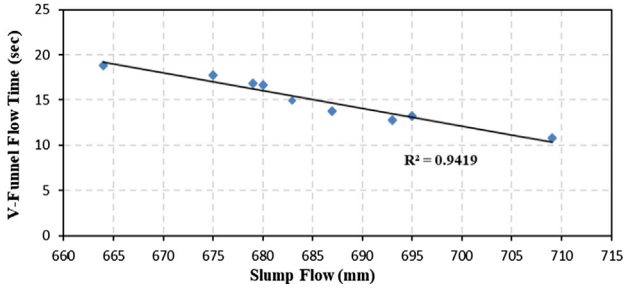

(a) Slump flow versus V-Funnel

Fig. 14. Relationship between the fresh properties of SCGC.

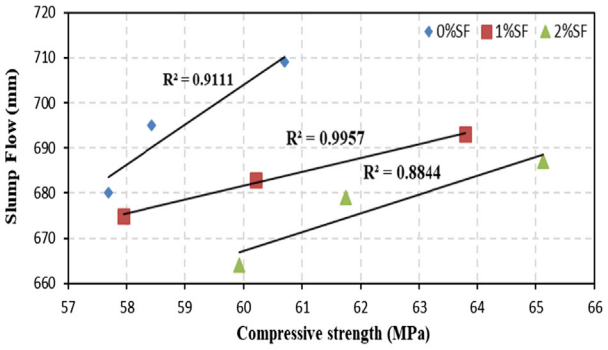

(a) Slump flow versus compressive strength

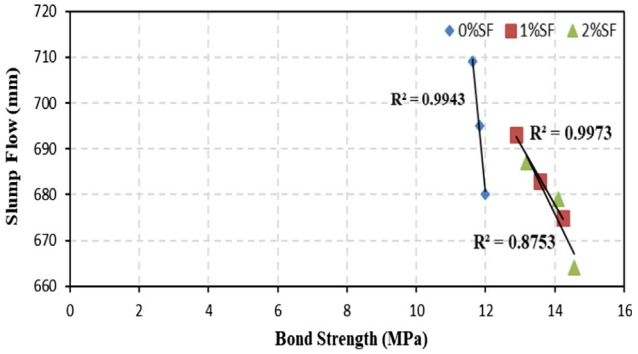

(b) Slump flow versus bond strength

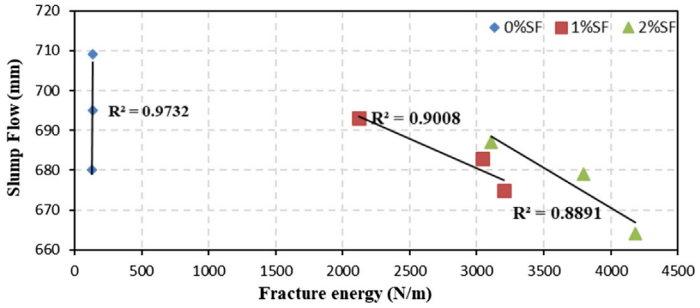

(c) Slump flow versus fracture toughness

Fig. 15. Relationship between the fresh properties and hardened properties of SCGC.

mance. The steel fibers also affected the fresh state performance; however, the effect of SF on the fresh state performance was found to be less than the effect of nano-silica. According to the results, nano-silica alone is not an effective parameter on fracture energy; however, when it is used with SF together, the positive influence of NS on the fracture energy can be seen clearly.

Gesoglu et al. [47] investigated the influence of silica fume and SF on the mechanical properties of ordinary concrete and they con-

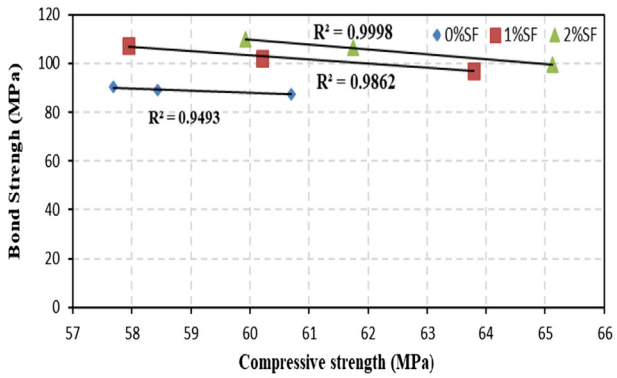

(a) Compressive strength vs bond strength

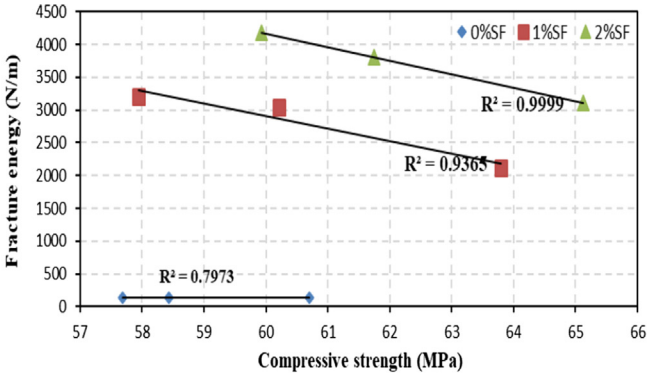

(b) Compressive strength vs fracture energy

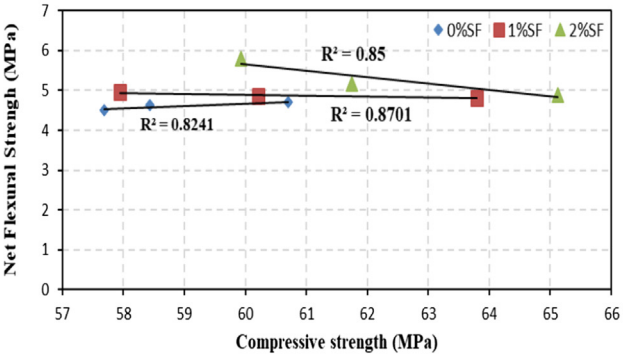

(c) Compressive strength vs flexural strength

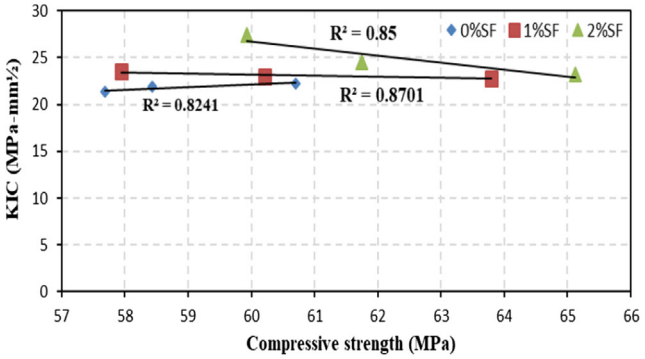

(d) Compressive strength vs KIC

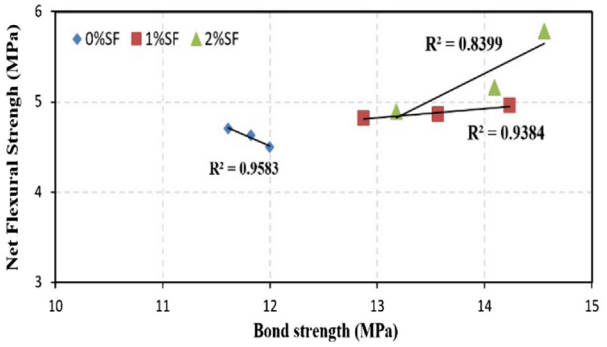

(e) Bond strength vs flexural strength

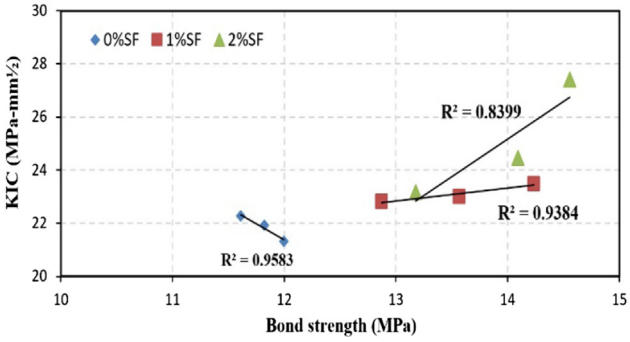

(f) Bond strength vs KIC

Fig. 16. Relationship between the hardened properties of SCGC.

cluded that SF volumes and types had no much more influence on compressive strength of specimens; however, SF effect was found to be effective on the bond strength and bending strength. It is concluded in current study that the simultaneous use of SF and NS reduces the fresh state performances; however, it improves the compressive strength, bond and flexural strengths of the SCGC specimens.

4. Conclusions

In this study, the combined influence of NS and SF on the fresh and hardened state performance of the self-compacting geopolymer concrete was investigated. The following results were obtained;

- Fresh state test results indicated that simultaneous use of nano-silica and steel fiber had negative effect on the slump flow diameter, t_{500} flow time, V-funnel flow time and L-Box passing ability. The highest reduction in the fresh performance was observed in the mixes including the highest amounts of NS (2%) and SF (1%). However, even in this case, the self-compacting geopolymer mixes satisfied the required flowability and passing ability criteria as specified by EFNARC specifications and TS 12350 standards.
- The higher nano-silica addition into the SCGC mixed improved the resistance to segregation and bleeding and the mixes including nano-silica were observed to be more cohesive than the mixes without NS.

Table 4
Statistical evaluation of the test result.

Dependent Variable	Independent variable	Sequential Sum of Squares	Mean Square	Computed F	P-Value	Significance	Contribution (%)
Slump flow diameter	Addition of steel fiber	494.0	247.0	26.46	0.005	Yes	36.6
	NS replacement level	818.67	409.33	43.86	0.002	Yes	60.6
	Error	37.33	9.33				2.8
	Total	1350					
Slump flow time (T_{500})	Addition of steel fiber	0.18047	0.090233	13.24	0.017	Yes	18.1
	NS replacement level	0.79207	0.396033	58.10	0.001	Yes	79.2
	Error	0.02727	0.006817				2.7
	Total	0.99980					
V- funnel flow time	Addition of steel fiber	12.5348	6.2674	37.43	0.003	Yes	23.1
	NS replacement level	41.1590	20.5795	122.90	0.000	Yes	75.7
	Error	0.6698	0.1674				1.2
	Total	54.3636					
L- Box height ratio	Addition of steel fiber	0.004289	0.002144	48.25	0.002	Yes	32.3
	NS replacement level	0.008822	0.004411	99.25	0.000	Yes	66.4
	Error	0.000178	0.000044				1.3
	Total	0.013289					
Compressive strength	Addition of steel fiber	16.605	8.3025	15.19	0.014	Yes	31.5
	NS replacement level	33.981	16.9904	31.08	0.004	Yes	64.4
	Error	2.186	0.5466				4.1
	Total	52.772					
Bond strength	Addition of steel fiber	439.79	219.897	45.14	0.002	Yes	79.6
	NS replacement level	93.27	46.637	9.57	0.030	Yes	16.9
	Error	19.49	4.872				3.5
	Total	552.55					
Fracture energy	Addition of steel fiber	20,544,913	10,272,457	93.17	0.000	Yes	94.1
	NS replacement level	841,437	420,718	3.82	0.118	No	3.9
	Error	441,037	110,259				2
	Total	21,827,387					

- V-funnel and slump flow results exhibited that all produced SCGC mixes were in the range of VS2/VF2 viscosity class, which has good bleeding and segregation resistance, and low formwork pressure according to EFNARC.
- The incorporation of nano-silica in the SCGC mixes slightly reduced the compressive strength, while the addition of steel fiber slightly improved the compressive strength of SCGC specimens. The decreasing effect of nano-silica on the compressive strength can be compensated with the steel fiber addition.
- The steel fiber enhanced the bond resistance, three-point bending strength, fracture toughness and stress intensity factor results of SCGC specimens due to the crack arresting capability of SF. Nano-silica does not have a contributing effect on flexural performance alone; however, when it is used with steel fibers together, bond strength, flexural strength and fracture properties of the specimens were enhanced significantly due to the better adhesion of NS. The superior mechanical performance was obtained for the specimens with the highest amounts of nano-silica (2%) and steel fiber (1%).
- Statistical analysis results showed that independent parameters were found to have an important influence on the fresh and hardened state properties of SCGC. The most influential parameters were found as the addition of nano-silica and steel fiber. The nano-silica addition was found to be more effective than the addition of steel fiber regarding both fresh state performances (slump flow, T500 flow time, V-Funnel flow time and L-Box ratio) and the compressive strength of the specimens. However, the incorporation of steel fiber was found to be the most effective factor on the bond strength and flexural performance of SCGC specimens.
- The nano-silica utilization with steel fibers on SCGC specimens affected the fresh state properties and compressive strength adversely, while the combined utilization of NS and SF significantly improved the flexural strength and fracture performance of SCGC specimens, which can be attributed to the crack bridging ability of steel fibers and better adhesion and bond strength of the nano-silica incorporation.

Conflict of interest

None.

References

[1] D. Hardjito, B.V. Rangan, Development and Properties of Low-calcium Fly Ash-based Geopolymer Concrete, Research Report GC1, Curtin University of Technology, Australia, 2005.
[2] B.V. Rangan, Low-Calcium, Fly-Ash-Based Geopolymer Concrete, Concr. Constr. Eng. Handb., Taylor Fr. Group, Boca Raton, FL, 2008.
[3] J. Temuujin, A. van Riessen, K.J.D. MacKenzie, Preparation and characterisation of fly ash based geopolymer mortars, Constr. Build. Mater. 24 (2010) 1906–1910.
[4] D.L.Y. Kong, J.G. Sanjayan, Damage behavior of geopolymer composites exposed to elevated temperatures, Cem. Concr. Compos. 30 (2008) 986–991, https://doi.org/10.1016/j.cemconcomp.2008.08.001.
[5] J. Davidovits, Geopolymers - Inorganic polymeric new materials, J. Therm. Anal. 37 (1991) 1633–1656, https://doi.org/10.1007/BF01912193.
[6] P. Duxson, A. Fernández-Jiménez, J.L. Provis, G.C. Lukey, A. Palomo, J.S.J. Van Deventer, Geopolymer technology: The current state of the art, J. Mater. Sci. 42 (2007) 2917–2933, https://doi.org/10.1007/s10853-006-0637-z.
[7] A. Nazari, F.P. Torgal, A. Cevik, J.G. Sanjayan, Compressive strength of tungsten mine waste-and metakaolin-based geopolymers, Ceram. Int. 40 (2014) 6053–6062.
[8] J. Davidovits, Geopolymer Chemistry and Applications, 2nd ed., Inst. Geopolymer, SaintQuentin, Fr., 2008.
[9] J. Davidovits, Geopolymer cement to minimize carbon-dioxde greenhouse-warming, Ceram. Trans. 37 (1993) 165–182.
[10] D. Hardjito, S.E. Wallah, D.M.J. Sumajouw, B.V. Rangan, On the development of fly ash-based geopolymer concrete, Mater. J. 101 (2004) 467–472.
[11] A. Nazari, J.G. Sanjayan, Modelling of compressive strength of geopolymer paste, mortar and concrete by optimized support vector machine, Ceram. Int. 41 (2015) 12164–12177.
[12] F. Ahmed Memon, M.F. Nuruddin, S. Demie, N. Shafiq, Effect of curing conditions on strength of fly ash-based self-compacting geopolymer concrete, Int. J. Civ. Environ. Eng. 3 (2011) 183–186.

[13] F.A. Memon, F. Nuruddin, N. Shafiq, Compressive strength and workability characteristics of low-calcium fly ash-based self-compacting geopolymer concrete, Int. J. Civ. Environ. Eng. 3 (2011) 72–78.
[14] A. Noushini, A. Castel, The effect of heat-curing on transport properties of low-calcium fly ash-based geopolymer concrete, Constr. Build. Mater. 112 (2016) 464–477, https://doi.org/10.1016/j.conbuildmat.2016.02.210.
[15] E.P. Koehler, Aggregates in Self-Consolidating Concrete, Doctoral Dissertation, 2007.
[16] H.A.F. Dehwah, Mechanical properties of self-compacting concrete incorporating quarry dust powder, silica fume or fly ash, Constr. Build. Mater. 26 (2012) 547–551, https://doi.org/10.1016/j.conbuildmat.2011.06.056.
[17] O. Boukendakdji, S. Kenai, E.H. Kadri, F. Rouis, Effect of slag on the rheology of fresh self-compacted concrete, Constr. Build. Mater. 23 (2009) 2593–2598, https://doi.org/10.1016/j.conbuildmat.2009.02.029.
[18] M. Tamil Selvi, T.S. Thandavamoorthy, Mechanical and durability properties of steel and polypropylene fibre reinforced concrete, Int. J. Earth Sci. Eng. 7 (2014) 696–703.
[19] A. Khaloo, E.M. Raisi, P. Hosseini, H. Tahsiri, Mechanical performance of self-compacting concrete reinforced with steel fibers, Constr. Build. Mater. 51 (2014) 179–186, https://doi.org/10.1016/j.conbuildmat.2013.10.054.
[20] O. Gencel, W. Brostow, T. Datashvili, M. Thedford, Workability and mechanical performance of steel fiber-reinforced self-compacting concrete with fly ash workability and mechanical performance of steel concrete with fly ash, Compos. Interfaces 18 (2011) 169–184, https://doi.org/10.1163/092764411X567567.
[21] C. Frazão, A. Camões, J. Barros, D. Gonçalves, Durability of steel fiber reinforced self-compacting concrete, Constr. Build. Mater. 80 (2015) 155–166, https://doi.org/10.1016/j.conbuildmat.2015.01.061.
[22] M.F. Ahmed, M.F. Nuruddin, N. Shafiq, Compressive strength and workability characteristics of low-calcium fly ash-based self-compacting geopolymer concrete, Int. J. Civil, Environ. Struct. Constr. Archit. Eng. 5 (2011) 64–70.
[23] M. di Prisco, R. Felicetti, F. Iorio, R. Gettu, On the identification of SFRC tensile constitutive behaviour, Fract. Mech. Concr. Struct. AA Balkema Publ. Rotterdam (2001) 541–548.
[24] F.N. Okoye, S. Prakash, N.B. Singh, Durability of fly ash based geopolymer concrete in the presence of silica fume, J. Clean. Prod. 149 (2017) 1062–1067.
[25] T. Tho-In, V. Sata, K. Boonserm, P. Chindaprasirt, Compressive strength and microstructure analysis of geopolymer paste using waste glass powder and fly ash, J. Clean. Prod. 172 (2018) 2892–2898.
[26] X.Y. Zhuang, L. Chen, S. Komarneni, C.H. Zhou, D.S. Tong, H.M. Yang, W.H. Yu, H. Wang, Fly ash-based geopolymer: clean production, properties and applications, J. Clean. Prod. 125 (2016) 253–267.
[27] S. Moukannaa, M. Loutou, M. Benzaazoua, L. Vitola, J. Alami, R. Hakkou, Recycling of phosphate mine tailings for the production of geopolymers, J. Clean. Prod. 185 (2018) 891–903.
[28] W. Hu, Q. Nie, B. Huang, X. Shu, Q. He, Mechanical and microstructural characterization of geopolymers derived from red mud and fly ashes, J. Clean. Prod. 186 (2018) 799–806.
[29] F.A. Memon, M.F. Nuruddin, S. Khan, N. Shafiq, T. Ayub, Effect of sodium hydroxide concentration on fresh properties and compressive strength of self-compacting geopolymer concrete, J. Eng. Sci. Technol. 8 (2013) 44–56.
[30] S. Iqbal, A. Ali, K. Holschemacher, T.A. Bier, Effect of change in micro steel fiber content on properties of high strength steel fiber reinforced lightweight self-compacting concrete (HSLSCC), Proc. Eng. 122 (2015) 88–94, https://doi.org/10.1016/j.proeng.2015.10.011.
[31] R. Dubey, P. Kumar, Effect of superplasticizer dosages on compressive strength of self compacting concrete, Int. J. Civ. Struct. Eng. 3 (2012) 360–366, https://doi.org/10.6088/ijcser.201203013034.
[32] M.F. Nuruddin, S. Demie, M.F. Ahmed, N. Shafiq, M. Fareed Ahmed, M. Fadhil Nuruddin, Effect of superplasticizer and NaOH molarity on workability, compressive strength and microstructure properties of self-compacting geopolymer concrete, World Acad. Sci. Eng. Technol. 74 (2011) 8–14, https://doi.org/10.1139/l11-077.
[33] V. Corinaldesi, G. Moriconi, Characterization of self-compacting concretes prepared with different fibers and mineral additions, Cem. Concr. Compos. 33 (2011) 596–601, https://doi.org/10.1016/j.cemconcomp.2011.03.007.
[34] M. Olivia, H. Nikraz, Properties of fly ash geopolymer concrete designed by Taguchi method, Mater. Des. 36 (2012) 191–198, https://doi.org/10.1016/j.matdes.2011.10.036.
[35] EFNARC, The European Guidelines for Self-Compacting Concrete: Specification, Production and Use, Eur. Guidel. Self Compact. Concr. 68 (2005).
[36] ASTM C39/C39M-01, Standard test method for compressive strength of cylindrical concrete specimens, Am. Soc. Test. Mater., West Conshohocken, USA, 2003.
[37] RILEM RC 6, Recommendations for the testing and use of constructions materials bond test for reinforcement steel. 2. Pull-out test, 1996.
[38] F.M.C.D. Recommendation, T. Recommendation, Draft recommendation: "Determination of the fracture energy of mortar and concrete by means of three-point bend tests on notched beams, Mater. Struct. 18 (1985) 484, https://doi.org/10.1007/BF02498757.
[39] B. Akcay, M.A. Tasdemir, Optimisation of using lightweight aggregates in mitigating autogenous deformation of concrete, Constr. Build. Mater. 23 (2009) 353–363, https://doi.org/10.1016/j.conbuildmat.2007.11.015.
[40] P.E. Peterson, Fracture energy of concrete: Method of determination, Cem. Concr. Res. 10 (1980) 79–89, https://doi.org/10.1016/0008-8846(80)90054-X.
[41] B. 12350-8 EN, Testing self compacting concrete: slump flow test, Br. Stand. Int. (2010).
[42] B. 12350-9 EN, Testing self compacting concrete: V-Funnel Test, Br. Stand. Int. (2010).
[43] B. 12350–10 EN, Testing self compacting concrete: L-box test, Br. Stand. Int. (2010).
[44] J.S. Belkowitz, W.L.B. Belkowitz, K. Nawrocki, F.T. Fisher, Impact of nanosilica size and surface area on concrete properties, ACI Mater. J. 112 (2015) 419–427, https://doi.org/10.14359/51687397.
[45] A. Çevik, R. Alzeebaree, G. Humur, A. Niş, M.E. Gülşan, Effect of nano-silica on the chemical durability and mechanical performance of fly ash based geopolymer concrete, Ceram. Int. (2018), https://doi.org/10.1016/j.ceramint.2018.04.009.
[46] M. Nili, V. Afroughsabet, Combined effect of silica fume and steel fibers on the impact resistance and mechanical properties of concrete, Int. J. Impact Eng. 37 (2010) 879–886.
[47] M. Gesoğlu, E. Güneyisi, R. Alzeebaree, K. Mermerdaş, Effect of silica fume and steel fiber on the mechanical properties of the concretes produced with cold bonded fly ash aggregates, Constr. Build. Mater. 40 (2013), https://doi.org/10.1016/j.conbuildmat.2012.11.074.
[48] E. Güneyisi, M. Gesoğlu, A. Mohamadameen, R. Alzeebaree, Z. Algin, K. Mermerdaş, Enhancement of shrinkage behavior of lightweight aggregate concretes by shrinkage reducing admixture and fiber reinforcement, Constr. Build. Mater. 54 (2014), https://doi.org/10.1016/j.conbuildmat.2013.12.041.
[49] E. Baran, T. Akis, S. Yesilmen, Pull-out behavior of prestressing strands in steel fiber reinforced concrete, Constr. Build. Mater. 28 (2012) 362–371.
[50] T. Abu-Lebdeh, S. Hamoush, W. Heard, B. Zornig, Effect of matrix strength on pullout behavior of steel fiber reinforced very-high strength concrete composites, Constr. Build. Mater. 25 (2011) 39–46.
[51] N. Krstulovic-Opara, K.A. Watson, J.M. LaFave, Effect of increased tensile strength and toughness on reinforcing-bar bond behavior, Cem. Concr. Compos. 16 (1994) 129–141.
[52] M.H. Harajli, K.A. Salloukh, Effect of fibers on development/splice strength of reinforcing bars in tension, Mater. J. 94 (4) (1997) 317–324.
[53] P.K. Sarker, R. Haque, K.V. Ramgolam, Fracture behaviour of heat cured fly ash based geopolymer concrete, Mater. Des. 44 (2013) 580–586, https://doi.org/10.1016/j.matdes.2012.08.005.